ELSEVIER

Polymer 43 (2002) 6527–6534

polymer

www.elsevier.com/locate/polymer

The effects of end groups on thermodynamics of polymer blends III LCST phase diagrams

Paul A. Schacht[1], Jeffrey T. Koberstein*

Department of Chemical Engineering and The Polymer Program, Institute of Materials Science, University of Connecticut, Storrs, CT 06269-3136, USA

Received 22 July 2002; accepted 25 July 2002

Abstract

The effect of end group substitution on the phase behavior of blends of poly(styrene) (PS) and poly(vinyl methyl ether) (PVME) is characterized by determination of experimental cloud point curves. Incorporation of a fluorosilane end group on PS increases the lower critical solution temperature by 10 °C indicating enhanced miscibility. The end group effect is modeled by a modification of Sanchez–Lacombe–Balazs (SLB) theory that employs binary interaction theory to account for the end group effect. The increased miscibility is quantitatively predicted by the modified theory when binary interaction parameters are calculated by group contribution methods. SLB theory is also compared to phase diagrams of PS/PVME blends previously reported by Halary et al., and Yang et al., but fails to reproduce the observed behavior over the entire molecular weight range. Optimal fits of these data yield interaction energy parameters that are molecular weight dependent, suggesting that the SLB theory may require molecular weight dependent equation of state parameters in order to reproduce the phase behavior of polymer blends. © 2002 Published by Elsevier Science Ltd.

Keywords: Polymer blends; Polystyrenes; End group

1. Introduction

The first two papers in this series examined the effects of end group modification on the interfacial tension [1] and phase behavior [2] of immiscible binary homopolymer blends characterized by the existence of an upper critical solution temperature. The critical temperatures were found to differ by as much as 150 °C for blends of poly(isoprene) with α,ω-functional poly(dimethylsiloxanes) (PDMS) having the following three end groups: a trimethylsilyl control (PDMS–CH_3), aminopropyl (PDMS–NH_2), and carboxypropyl (PDMS–COOH). We found that the general increase in miscibility due to end group substitution could be reproduced by a modified Flory–Huggins free energy expression in which the end group interactions were accounted for by binary interaction theory (BIT) [3–5]. The same approach was found to be successful in modeling end group effects in polyester–polycarbonate blends [6] and in explaining (see Ref. [2]) the reported absence of end group effects [7] on the phase diagrams of α,ω-hydroxy and trimethylsilyl functional poly(dimethylsiloxane) blended with poly(methylphenylsiloxane) (PMPS). Additional reports of end group effects on polymer blend properties have also appeared [8–10].

In the report that follows, we present an experimental and theoretical investigation of end group effects on the phase behavior of a polymer blend exhibiting a lower critical solution temperature (LCST). The LCST blend of polystyrene and poly(vinyl methyl ether) (PS/PVME) is selected for study, in part, because its phase behavior is well documented [11–21]. Polystyrene is also convenient for the investigation of end group effects because end-functional polystyrenes of narrow molecular weight distribution and with a variety of end groups may be readily prepared by standard anionic synthesis methods.

The PS/PVME blend system is also advantageous from the theoretical point of view, because its phase behavior is reported to be well-represented by the Sanchez–Lacombe–Balazs (SLB) modified fluid lattice theory [22]. SLB theory provides a versatile foundation for modeling the phase behavior of LCST blends containing end-functional

* Corresponding author. Address: Department of Chemical Engineering and Applied Chemistry, Columbia University, MC 4721, 500 West 120th Street, New York, NY 10027, USA. Tel.: +1-212-854-3120; fax: +1-212-854-3054.

E-mail address: jk1191@columbia.edu (J.T. Koberstein).

[1] Present address: Advanced Elastomer Systems, L.P., 1000 Seville Road, Wadsworth, OH 44281, USA.

0032-3861/02/$ - see front matter © 2002 Published by Elsevier Science Ltd.
PII: S0032-3861(02)00539-6

Table 1
Characteristics of polymers studied

Polymer	Sample	M_w	M_n	M_w/M_n
Fluorosilane-terminated poly(styrene)	PSF	36,847	31,109	1.18
Proton-terminated poly(styrene)	PSH	31,732	28,396	1.12
Poly(vinyl methyl ether)	PVME	99,000	46,698	2.12

polymers because it accounts for finite compressibility effects and separates the contributions of non-specific and specific interactions by using two adjustable energy terms: a mer–mer interaction energy, ε^*_{12}, and an additional energy, $\delta\varepsilon$, due to specific interactions. Since specific interactions are treated separately, group contribution methods [23] can be employed to estimate the mer–mer interaction energies between the end group and backbone units. End group effects can subsequently be accounted for by a straightforward application of BIT [3–5] assuming that an end-functional homopolymer behaves as a statistical copolymer.

The present paper compares the phase behavior of a control system of proton terminated polystyrene (PSH) blended with PVME to that of a blend containing end-functional polystyrene (PSF) terminated with a fluorosilane end group, $Si(CH_3)_2(CH_2)_2(CF_2)_5CF_3$. Phase diagrams for the two PS/PVME systems are determined by cloud point experiments and are modeled by application of the SLB theory that is modified to account for end group effects. We demonstrate that this modified theoretical framework provides an excellent representation of the phase behavior of these LCST blends containing an end-functional polymer.

2. Experimental

The end-functional polystyrenes were synthesized anionically by Dr Michael A. Drzewinski[2] of EniChem America Inc. using cyclohexane as the major solvent (with minor addition of tetrahydrofuran) and *sec*-butyllithium as the initiator. Prior to termination, the living polystyryl lithium was split into two equal batches. The control polystyrene, PSH, was methanol quenched to yield the typical proton end group, whereas the remaining batch, PSF, was terminated with a chlorofluorosilane to attach the fluorosilane end group, $Si(CH_3)_2(CH_2)_2(CF_2)_5CF_3$. This procedure ensures that the polymer backbone of PSH and PSF is identical. The fluorosilane functionality was determined by elemental analysis (Galbraith Laboratories) to be 66%. Table 1 summarizes size exclusion chromatography results for the three blend components performed using a Beckman Model 100A pump, Phenomenex Phenogel columns (2×30 cm^2, 5 μm mixed gel), an Altex Model 156 differential refractive index detector, and toluene as the solvent. The poly(vinyl methyl ether), obtained from Scientific Polymer Products, was used as received and dried under vacuum. X-ray photoelectron spectroscopy measurements confirmed that the PVME was free from carbonyl residues.

Blend films were prepared by solution casting ~5% (w/v) toluene solutions into 10×100 mm^2 Petri dishes. Following a 24 h period of air-drying in a fume hood, the blends were annealed at 60 °C under reduced pressure for about 48 h. Approximately 0.2 g of the blends was subsequently charged into cylindrical tubes (OD = 7 mm). The filled tubes were annealed for a period of 24–72 h prior to use at reduced pressure and at a temperature about 75 °C above the glass transition temperature of the blend. The final annealing step homogenizes the blend, removes dissolved gases, and serves to pre-equilibrate the blends by erasing previous thermal history. All blends were judged to be miscible, by their optical clarity, prior to the laser light transmission experiment.

Cloud point temperatures were determined by performing laser light transmission experiments using an apparatus built in-house. The incident beam from a 1 mW Melles–Griot helium–neon laser was defined by 1 mm channels within a cylindrical, aluminum heating block, passed through the sample and the transmitted intensity was detected with a photomultiplier tube (Hamamatsu) optimized for 632.8 nm radiation. An Omega CN2011J PID temperature controller (±1 °C) was used to control the heating rate (~2 °C/min for all experiments) and the sample is held continuously under vacuum. The cloud point temperature for each experiment was determined as the onset of a rapid decrease in the transmitted light intensity.

Each reported cloud point represents the average of 3–5 samples. The error bands on temperature result from the inherent ±1 °C error in thermocouple accuracy and intrinsic temperature variation within the apparatus. Although the true cloud point should be assessed by extrapolating to zero heating rate, Nishi and Kwei [15] showed that there is less than 3 °C variation in the cloud point temperature within a heating rate range of 1–10 °C/min. Therefore, extrapolation to zero heating rate was neglected. Reported error bars represent ±1 standard deviation. Errors in the blend composition are less than 4.0×10^{-4} g/g for all cases.

3. Results and analysis

Experimental cloud point curves for the PSH/PVME and PSF/PVME blends are shown in Fig. 1. The cloud point curve for the PSH/PVME system is fairly symmetric with an apparent critical point at 50% PVME and 144 °C. The PSF/PVME phase diagram, on the other hand, is flatter, making determination of the critical point more difficult. The critical temperature is approximately 154 °C and the corresponding critical composition lies in the range of 50–65% PVME. Since the PSH and PSF homopolymers have backbones of identical molecular weight, the approximate 10 °C increase

[2] The ρ^* value for PS was reset to the original value for protonated material.

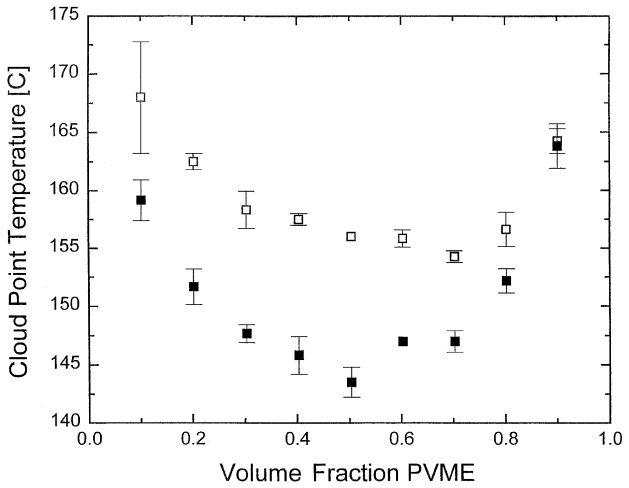

Fig. 1. Experimental cloud point curves for blends of PSH with PVME (filled squares) and PSF with PVME (open squares). Error bars indicate a range of two standard deviations.

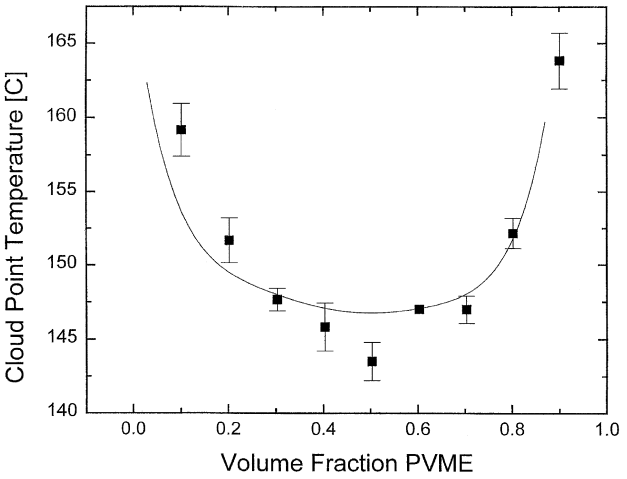

Fig. 2. Comparison of experimental (filled squares) and theoretical (line) phase diagrams for PSH/PVME blends. Error bars indicate a range of two standard deviations.

in LCST for the PSF/PVME system (indicating an increase in miscibility) can be attributed to the presence of the fluorosilane end group.

In order to gain a deeper understanding of the origin of improved miscibility upon incorporation of fluorosilane end groups onto PS, the cloud point curves were modeled with the SLB modified fluid lattice theory [22] using BIT [3–5] and group contribution methods to estimate binary interaction parameters, as detailed in Appendix. The SLB model has three adjustable parameters: q, a parameter related to the ratio of degeneracies of non-specific to specific interactions, and two energy parameters, ε^*_{vs}/k, and $\delta\varepsilon^*/k$. The strength of non-specific mer–mer interactions between PS and PVME is represented by the value of ε^*_{vs}, $\delta\varepsilon^*$ indicates the strength of specific interactions, and k is Boltzmann's constant. The three adjustable parameters are not wholly independent. Fix any one term and the other two become a coupled pair. A theoretical phase diagram for the PSH/PVME system was generated by first estimating a value of $\varepsilon^*_{vs}/k = 624.77$ K from group contribution/solubility parameter methods described in Appendix, and then regressing the theory to experimental data by minimization of the sum of least squares differences between the calculated spinodal temperatures and the experimentally determined cloud points. In performing the regression, ε^*_{vs}/k was held at 624.77 K while $\delta\varepsilon^*/k$ and q were varied. This is in contrast to the original SLB approach [22], wherein q was held constant while the parameters ε^*_{vs}/k and $\delta\varepsilon^*/k$ were varied. The optimization yielded $\delta\varepsilon^*/k = 749.22$ K and $q = 11$. Fig. 2 demonstrates that this procedure provides a reasonable match between theoretical spinodal temperatures and experimental cloud point temperatures for the PSH/PVME control system.

The set of optimal parameters determined for the PSH/PVME blend served as a basis for the calculation of the theoretical phase diagram for the PSF/PVME blend. The fluorosilane end group was assumed to have no effect on specific interactions, that is, q and $\delta\varepsilon^*/k$ were fixed to the optimal values found for the PSH/PVME blend: $q = 11$ and $\delta\varepsilon^*/k = 749.22$ K. The effect of the end groups was accounted for entirely within the term $\varepsilon^*_{vs,eff}/k$, which was adjusted in order to optimize the correspondence between theory and the experimental PSF/PVME cloud point data.

The optimal value of $\varepsilon^*_{vs,eff}/k$ obtained for the PSF/PVME blend, 618.06 K, reproduced well the experimental cloud point curve as shown in Fig. 3. This value is lower than the optimal value of $\varepsilon^*_{vs}/k = 624.77$ K found for the PSH/PVME blend, consistent with increased miscibility for the PSF/PVME blends indicated by the cloud point data.

In previous studies [1,2], we demonstrated that BIT could be employed to successfully calculate the effects of end group substitution on interaction parameters. In the present case, our goal is to examine whether BIT can successfully predict the observed change in the non-specific interaction parameter upon end group substitution. Upon incorporation

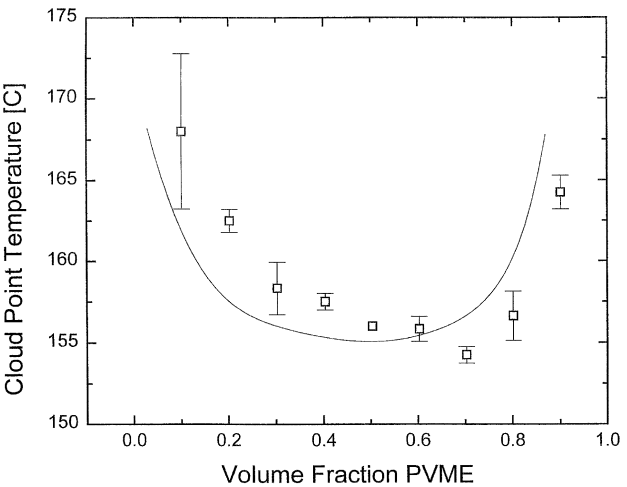

Fig. 3. Comparison of experimental (□) and predicted (—) phase diagrams for PSF/PVME blends. Error bars indicate a range of two standard deviations.

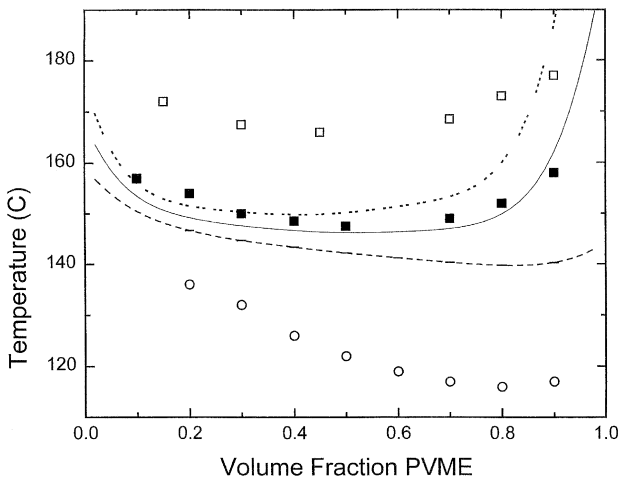

Fig. 4. Comparison of phase diagrams from Halary et al. [21] with the theory based on the optimized parameters from the PSH/PVME blends: $M_w = 20{,}000$ (□), $M_w = 36{,}000$ (■), $M_w = 233{,}000$ (○). The theoretical results are shown as lines: $M_w = 20{,}000$ (- - -); $M_w = 36{,}000$ (—); $M_w = 233{,}000$ (– – –).

of BIT into the SLB model, the effective cross interaction energy for non-specific interactions becomes

$$\varepsilon^*_{vs,eff} = \varepsilon^*_{vs} y_s + \varepsilon^*_{vf} y_f - \varepsilon^*_{sf} y_s y_f \quad (1)$$

where the subscripts v, s, and f refer to PVME, PS and the fluorinated end group, respectively, and the y_i are molar volume fractions for each species. In applying Eq. (1), a method is required for the estimation of both ε^*_{vf} and ε^*_{sf}. We choose to make these estimates from group contribution concepts described in Appendix. It is therefore useful to examine first whether group contribution concepts can predict the value of ε^*_{vs}/k found from regression of the PSH/PVME blend data. The group contribution prediction is $\varepsilon^*_{vs} = 648.31$ K, about 4% larger than the optimal regression value of 624.77 K. Group contribution methods therefore provide a reasonably accurate prediction of the non-specific interaction parameter between styrene and vinyl methyl ether.

In modeling the PSF/PVME blend data, group contribution methods are applied to estimate ε^*_{vs}, ε^*_{vf} and ε^*_{sf}. Incorporation of these values into BIT following Eq. (1) yields $\varepsilon^*_{vs,eff}/k = 642.11$ K, again about 4% larger than the optimal value $\varepsilon^*_{vs,eff}/k = 618.06$ K obtained by regression of the PSF/PVME data. Experimentally we find that introducing the fluorosilane end group reduces the effective mer–mer interaction energy by 1.1% whereas the BIT/group contribution approach predicts a 1.0% reduction. The agreement between predicted and measured non-specific interaction energies is encouraging considering that the calculations were based entirely upon tabulated group contribution data.

While the increased miscibility observed for the PSF/PVME system is consistent with the predictions of BIT, a possible complication is the potential immiscibility between end-functional and non-functional polystyrenes, since the end group functionality is only 66%. Calculations based on the group contribution estimates of solubility parameters show, however, that PSH and PSF should be miscible for all molecular weights and that incomplete polystyrene end group functionality should not affect the phase behavior of the PS/PVME blends. This result and the agreement between predicted and experimental values for $\varepsilon^*_{vs,eff}/k$ demonstrates that the BIT modified SLB theory is an effective tool for predicting the phase behavior of end-functional polymer blends.

The original SLB paper [22] suggested that, once a set of best fit parameters was obtained for a given polymer blend, the SLB theory could be used as a zero-adjustable-parameter predictive model. This conclusion, however, was based on the investigation of only two rather high molecular weight d-PS/PVME blends. To examine the validity of this conclusion more carefully, we have tested the zero-adjustable-parameter model with cloud point data published by Halary et al. [21] for five different PSH/PVME blends. From Fig. 4 (the results for two of the original blends have been omitted for sake of clarity), it is apparent that the zero-adjustable-parameter strategy does not adequately predict the correct phase behavior over the entire range of molecular weights. The fit to the PS ($M_w = 36$ K) data is a reasonably good one. This might be expected since the fitting parameters employed were obtained originally for a blend with PSH ($M_w = 32$ K). The cloud point curves for both the lowest and highest molecular weight blends, however, differ significantly from the theoretical predictions.

As an additional check of the zero-adjustable-parameter concept, data by Yang et al. [17] for a blend of deuterated polystyrene (dPS) ($M_w = 119$ K) with PVME ($M_w = 99$ K) was fit using the optimal parameter set of $\varepsilon^*_{12}/k = 666$ K, $\delta\varepsilon^*/k = 318.72$ K, and $q = 10$ at $z = 12$ (SLB Data Set 1: dPS, $M_w = 230$ K; PVME, $M_w = 389$ K [22]). Once again, as Fig. 5 shows, the correspondence is not acceptable. In the SLB zero-adjustable-parameter test case (SLB Data Set 2), the molecular weights of the components were 593 K for dPS and 1100 K for PVME, much larger than those employed by Yang et al.

In searching for an explanation for the poor predictability of molecular weight effects of the zero-adjustable parameter model, we realized that we should perhaps take into account the possible effects of the *sec*-butyl initiator fragment on anionically synthesized PS as an end group. To do this, the energy contribution of the butyl fragment was estimated using the solubility parameter approach as was done for the fluorosilane end group on PSF and we attempted to model the data of Halary et al., by using the BIT approach to reflect the effects of the butyl end group. This approach failed to reproduce the experimental results, however, and optimal energy parameters were consequently determined individually for each different molecular weight blend. Each of the Halary et al., blends was fit using the original SLB model (i.e. no BIT terms included) at constant $z = 12$ and $q = 11$

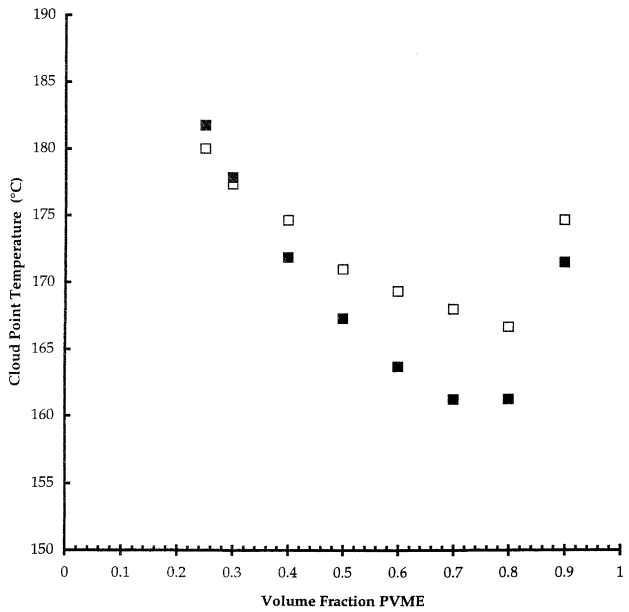

Fig. 5. Comparison of the experimental phase diagram by Yang et al. [17] (■) with theory (□) using optimal parameters reported by SLB for blends of perdeuterated PS with PVME.

while optimizing both ε_{12}^{*}/k and $\delta\varepsilon^{*}/k$. The optimal parameters are reported in Table 2. An inverse relationship between the two adjustable parameters is evident and both are clearly dependent on molecular weight.

The effect of end groups on bulk properties, such as yield strength, density, and surface tension, often scales inversely with the number average molecular weight [23,24]. The molecular weight dependence of the optimal ε_{vs}^{*}/k parameters was found to follow an empirical relation of form

$$\varepsilon_{vs}^{*}/k = 675.0 - 6350M_{n}^{-1.3} \quad (2)$$

The three-parameter equation in Eq. (2) (modeled using Origin for IBM compatible personal computers) suggests that the molecular weight dependence of ε_{vs}^{*}/k is similar to what would be expected for end group effects. We have shown, however, that consideration of the butyl end group effects cannot account for this behavior. The result indicates that the SLB theory, with a single set of equation of state parameters, cannot fully reproduce the phase behavior of PS/PVME blends, especially at low molecular weight. Sanchez noted that system compressibility effects greatly overpower the specific interaction character of a blend in the SLB model [22]. Since chain free volume is linked directly to compressibility, any changes due to molecular weight would be readily apparent in the PVT density measurements. The equation of state parameters, T^{*}, P^{*}, and ρ^{*} required for the SLB theory would therefore need to be molecular weight dependent in order for the theory to reproduce all of the experimental observations.

Table 2
Optimal energy parameters for Halary et al. data

M_n (g/mol)	ε_{12}^{*}/k (K)	$\delta\varepsilon^{*}/k$ (K)
19,300	541.1	1443.4
34,000	605.4	922.7
62,000	649.8	509.0
100,000	663.1	373.1
220,000	665.5	348.2

4. Conclusions

Experimental cloud point measurements on polymer blends exhibiting lower critical temperature phase behavior demonstrate that blend miscibility can be influenced by the nature of the chain end groups. Incorporation of a fluorosilane end group onto the polystyrene provided enhanced miscibility toward polyvinyl methyl ether as indicated by an increase in the LCST of about 10 °C. The increase in miscibility was successfully accounted for by a modification of the SLB fluid lattice model that employed BIT to calculate the effect of end groups on the non-specific interaction energy and group contribution methods to estimate mer–mer interaction energies between the blend constituents.

The SLB theoretical framework was also applied to model previously reported phase behavior for a number of PS/PVME blends. The optimal mer–mer interaction energies were found to increase with molecular weight, indicating that molecular weight dependent equation of state parameters may be required for the SLB theory to quantitatively reproduce the phase behavior of PS/PVME polymer blends.

Acknowledgements

This material is based on the work supported by, or in part by, the US Army Research Office and grant number DAAH04-95-1-0592 and the Polymers Program of the National Science Foundation (DMR-9502977 and DMR-9810069). The authors wish to thank Dr Michael A. Drzewinski for synthesizing the PS-F.

Appendix

The Solver Add-In for a Microsoft Excel 4.0 spreadsheet (for the Apple Macintosh) was employed to evaluate the spinodal by solution of the modified SLB equations. The Solver options used included Newton's search method with tangent estimates and forward derivative modes using a precision greater than 1×10^{-12} and a tolerance of 0.05. The sum of least squares residuals between the calculated and experimental spinodal temperatures was minimized by constraining the temperature at each experimental point (i.e. composition and temperature) in order to make the determinant in Eq. (A8) that follows go to zero.

Table A1
Equation of state parameters and reduced chain lengths

Component	T^* (K)	P^* (atm)	ρ^* (gm/cm^3)	r_i
PVME	657	3580	1.100	5976
PSH	735	3530	1.105	1681
PSF	735	3530	1.105	1952

The SLB model involves four parameters: z, q, ε_{12}^*, and $\delta\varepsilon^*$. However, as Sanchez pointed out, the lattice coordination number, z, is simply a scaling factor; therefore, once a value is assigned, z is no longer considered adjustable. The remaining three parameters are not wholly independent; fix any one term, and the other two become a coupled pair.

The SLB equation of state [22] relates the reduced density, $\tilde{\rho}$, of a mixture at temperature, T, to an average reduced chain length parameter, r, and an interaction energy parameter, ε_T^*. The reduced density, $\tilde{\rho}$, of the mixture represents the fraction of occupied sites on the lattice and is given by

$$\frac{\tilde{\rho}^2\varepsilon_T^*}{kT} + \ln(1-r) = \frac{1-r}{r} \tag{A1}$$

where k is Boltzmann's constant. The composition dependent size parameter, r, is defined in terms of the volume fraction ϕ_i of each component

$$\frac{1}{r} = \frac{\phi_1}{r_1} + \frac{\phi_2}{r_2} \tag{A2}$$

and the pure component reduced chain length of each blend constituent

$$r_i = \frac{M_w P_i^*}{RT_i^*\rho_i^*} \tag{A3}$$

where R is the gas constant M_w is the weight averaged molecular weight, and P_i^*, T_i^* and ρ_i^* are equation of state parameters for pure component, i.

A convenient feature of the theoretical framework for the present context is that the interaction energy parameter is separated into a term representing the non-specific mer–mer interactions, ε_{ij}^*, and a second term, $\delta\varepsilon$, that indicates the strength of specific interactions. The equation defining these interaction energies is

$$\varepsilon_T^* = \phi_1^2\varepsilon_{11}^* + 2\phi_1\phi_2 f_{12}^* + \phi_2^2\varepsilon_{22}^* \tag{A4}$$

where

$$f_{12}^* = \frac{z}{2}\left(\varepsilon_{12} + \delta\varepsilon - \frac{1}{kT}\ln\left[\frac{1+q}{1+q\mathrm{e}^{-\delta\varepsilon/kT}}\right]\right) \tag{A5}$$

The lattice coordination number, z, is a scaling factor for both enthalpy and entropy, and is arbitrarily set equal to 12 [22]. As can be seen from Eq. (A5), the two contributions to the mer–mer interactions between unlike species are: $\varepsilon_{12}^* \equiv \varepsilon_{12}z/2$, the magnitude of non-specific interactions, and $\delta\varepsilon^* \equiv z\delta\varepsilon/2$, the magnitude of specific interactions. The parameter, q, is related to the ratio of degeneracies of non-specific to specific interactions through the relation

$$\frac{\text{non-specific interactions}}{\text{specific interactions}} = q\mathrm{e}^{-\delta\varepsilon/kT} \tag{A6}$$

The free energy (J/mol) for the SLB model may be expressed as

$$f = -\tilde{\rho}\varepsilon_T^* - kT \times\left[\frac{\phi_1}{r_1}\ln(\phi_1) + \frac{\phi_2}{r_2}\ln(\phi_2) + \frac{(1-\tilde{\rho})}{\tilde{\rho}}\ln(1-\tilde{\rho}) + \frac{\ln(\tilde{\rho})}{r}\right] \tag{A7}$$

Theoretical phase diagrams were determined by solving for the spinodal curves using the SLB theory. As Sanchez showed, the second composition derivative of the free energy expression in Eq. (A7) can be derived using ordinary differential calculus.

$$\frac{\mathrm{d}^2 f}{\mathrm{d}\phi^2} = \begin{vmatrix} f_{\phi\phi} & f_{\phi\tilde{\rho}} \\ f_{\tilde{\rho}\phi} & f_{\tilde{\rho}\tilde{\rho}} \end{vmatrix} f_{\tilde{\rho}\tilde{\rho}}^{-1} \tag{A8}$$

where the partial derivatives ($f_{\phi\phi} = \partial^2 f/\partial\phi^2$, $f_{\phi\tilde{\rho}} = \partial^2\phi/\partial\phi\,\partial\tilde{\rho}$, and $f_{\tilde{\rho}\tilde{\rho}} = \partial^2 f/\partial\tilde{\rho}^2$) are taken by holding all other variables constant. The spinodal conditions are obtained when the determinant in Eq. (A8) is zero. In order to numerically assess the determinant, equation of state parameters for each component are required. The values adopted for the characteristic temperatures (T^*), pressures (P^*), and mass densities (ρ^*) are those used by Sanchez [22] and are listed in Table A1.[2]

The spinodal for the PSF/PVME blend containing end-functional homopolymer was calculated assuming a pseudo-binary system with free energy given by Eq. (A7), and neglecting the possible influence of end groups on the equation of state parameters. The effects of end groups on the interaction energy parameters were taken into account by considering the end group to be a third component. In doing so, we took advantage of the fact that SLB separates interaction energy contributions due to specific and non-specific interactions. We assumed that the end group does not affect the specific interactions and set $\delta\varepsilon^*$ equal to the optimal value obtained by regression of the data for the PSH/PVME blend.

The effect of the third component, the end group, on non-specific interactions was accounted for by application of BIT, which had been previously applied to model the interactions between a homopolymer and a random copolymer [3–5]. In effect, we assumed that the end-functional homopolymer behaves like a random copolymer, a reasonable assumption if the end group is randomly mixed within the blend in the miscible state.

Upon incorporation of BIT into the SLB model, the effective cross interaction energy for non-specific

Table A2
Characteristic parameter estimates for blend constituents

Constituent	Molar volume V (cm^3/mol)	Solubility parameter δ $[(J/cm^3)^{1/2}]$	T^* (K)	Volume fraction y
PVME homopolymer	57.60	17.76	571.31	–
PS backbone	90.95	20.15	735.68	0.991
Fluorosilane end group	227.8	15.09	412.49	0.006
sec-Butyl end group	71.9	16.76	508.72	0.003

interactions (i.e. ε^*_{12} in Eq. (A5)) becomes

$$\varepsilon^*_{vs,eff} = \varepsilon^*_{vs} y_s + \varepsilon^*_{vf} y_f - \varepsilon^*_{sf} y_s y_f \quad (A9)$$

where the subscripts v, s, and f refer to PVME, PS and the fluorinated end group, respectively, and the y_i are molar volume fractions for each species. The molar volume fraction of the end group, for example, is defined as

$$y_f = \frac{x_f V_f}{x_f V_f + V_b + n_s V_s} \quad (A10)$$

where x_f represents the fraction of chains with the fluorosilane end group ($x_f = 0.66$), n_s is the degree of polymerization for PS ($n_s = 272$), and the V_i are the component molar volumes. The subscript 'b' refers to the *sec*-butyl initiator fragment $CH_3CH_2CH(CH_3)-$ that constitutes one of the PS chain ends.

The molar volumes used for PVME [15] and PS [25] were 55.47 and 98.00 cm^3/mol, respectively. These values were determined experimentally for each monomer repeat unit. A group contribution method [25] was also used to estimate the molar volume of the two backbones, the fluorosilane end group, and the *sec*-butyl initiator fragment on the polystyrene. Several assumptions were made in calculations for the fluorosilane end group $—Si(CH_3)_2(CH_2)_2(CF_2)_5CF_3$. The volume of the $—CF_2—$ group was estimated by taking the difference between the $—CHF—$ and $—CH_2—$ groups ($19.85 - 16.45 = 3.4$) and adding it to the $—CHF—$ group volume ($19.85 + 3.4 = 23.25$ cm^3/mol). Similarly, the volume of the $—CF_3$ group was estimated by multiplying that difference by three and adding it to the $—CH_3$ value ($22.8 + 3 \times 3.4 = 33.00$ cm^3/mol)). The group contribution molar volume for the silicon atom is listed as zero [25]. Table A2 summarizes the solubility parameter and molar volume calculations for each component.

To utilize the BIT modified SLB theory as a predictive tool, a method for estimating these binary interaction energies is required. Since, both ε^*_{ii} and the solubility parameter, δ_i, are measures of a component's cohesive energy, a logical choice is to use well established group contribution methods for these estimations [25]. The solubility parameter was estimated from the molar volume, V_j, and tabulated molar attraction constants, F_j, for each chemical group moiety j within the unit under consideration according to the relation

$$\delta_i = \sum_j \left(\frac{F_j}{V_j}\right) \ (J/cm^3)^{1/2} \quad (A11)$$

The solubility parameter and the pure component interaction energy ε^*_{ii} differ only by a reference volume similar to the one implemented in Flory's rigid lattice theory [26] (where the unit volume of smallest component is usually designated as the V_{ref}). A variety of methods were considered to determine an appropriate reference volume: experimentally determined monomer molar volumes, group contribution table estimates of monomer molar volumes, and the pure component PVT characteristic data based on an ideal gas law type expression. Since the reduced chain length parameter, r, in the SLB theory is based on the equation of state parameters, the PVT approach was adopted to calculate the PVME unit volume (from PVME data in Table 2) as

$$V_{ref} = RT^*/P^* = 15.06 \ (cm^3/mol) \quad (A12)$$

Dimensional analysis of ε^*_{ii} leads to its relation to the solubility parameter.

$$\frac{\varepsilon^*_{ii}}{k} = T^*_i = \frac{\delta_i^2 V_{ref}}{R} \ (K) \quad (A13)$$

The pure component interaction energies were estimated from this relationship and group contribution estimates of the solubility parameters. Manipulation of Eq. (A13) leads to

$$P^*_i = K\delta_i^2 \ (atm) \quad (A14)$$

where P^* is measured in atmospheres, δ_i [in $(J/cm^3)^{1/2}$] and K is a known unit conversion factor. This relation is consistent with the direct determination of P^*_i by experimental cohesive energy density measurements [27]. Thus there exist several methods that allow for prediction of both pure component and BIT modified energy parameters for use in conjunction with the SLB model.

An estimate of the ε^*_{ij} cross term can be obtained from Hildebrand's solubility parameter concepts [28]. Assuming that the two components act like spherical particles, the mer–mer interaction parameter, ε^*_{ij}/k, is equal to the geometric mean of the pure component characteristic temperatures. Accepting this assumption leads to the

following expressions for the cross interaction energy

$$\frac{\varepsilon_{ij}^{*}}{k} = (T_i^{*}T_j^{*})^{0.5} = \frac{\delta_i\delta_j V_{\mathrm{ref}}}{R} = \frac{(P_i^{*}P_j^{*})^{1/2}V_{\mathrm{ref}}}{R_{\mathrm{gas}}} \ \mathrm{(K)} \qquad \text{(A15)}$$

With the interaction energies defined in terms of BIT and solubility parameters estimated by group contribution methods, the BIT modified SLB theory can be compared directly to experimental cloud point data for blends with end-functional homopolymers.

References

[1] Fleischer CA, Koberstein JT, Krukonis V, Wetmore P. Macromolecules 1993;26:4172.
[2] Lee M, Fleischer CA, Morales AR, Koberstein JT. Polymer 2001;42:9163.
[3] ten Brinke G, Karasz FE, MacKnight WJ. Macromolecules 1983;16:1827.
[4] Kambour RP, Bendler J, Bopp RC. Macromolecules 1983;16:753.
[5] Paul DR, Barlow JW. Polymer 1984;25:487.
[6] Kollodge JS, Porter RS. Macromolecules 1995;28:4097.
[7] Kuo CM, Clarson SJ. Eur Polym J 1993;29:661.
[8] Min KE, Chiou JS, Barlow JW, Paul DR. Polymer 1987;28:1721.
[9] Callaghan TA, Paul DR. J Polym Sci Part B Polym Phys 1994;32:1813.
[10] Callaghan TA, Paul DR. J Polym Sci Part B Polym Phys 1994;32:1847.
[11] Bank M, Leffingwell J, Thies C. Macromolecules 1971;4:43.
[12] Bank M, Leffingwell J, Thies C. J Polym Sci Part A-2 1972;10:1097.
[13] Kwei T, Kl Nishi Tl, Roberts RF. Macromolecules 1974;7:667.
[14] Nishi T, Wang T, Kwei TK. Macromolecules 1975;8:227.
[15] Nishi T, Kwei TK. Polymer 1975;6:285.
[16] Gelles R, Frank C. Macromolecules 1982;15:1486.
[17] Yang H, Shibayama M, Stein RS, Shimizu N, Hashimoto T. Macromolecules 1986;19:1667.
[18] Park H, Pearce EM, Kwei TK. Macromolecules 1990;23:434.
[19] Halary JL, Ubrich JM, Monnerie L, Yang H, Stein RS. Polym Commun 1985;26:73.
[20] Ben Cheikh Larbi F, Leloup S, Halary JL, Monnerie L. Polym Commun 1986;27:23.
[21] Halary JL, Ubrich JM, Nunzi JM, Monnerie L, Stein RS. Polymer 1984;25:957.
[22] Sanchez IC, Lacombe R, Balazs AC. Macromolecules 1989;22:2325.
[23] Fox TG, Flory PJ. J Polym Sci 1954;14:315.
[24] Fox TG, Loshaek S. J Polym Sci 1955;15:371.
[25] Van Krevelen DW. Properties of polymers: their estimation and correlation with chemical structure. Amsterdam: Elsevier; 1976.
[26] Flory PJ. Principles of polymer chemistry. Ithaca, NY: Cornell University Press; 1953.
[27] Sanchez IC. In: Meyers RA, editor. Encyclopedia of physical science and technology, vol. 11. Orlando: Academic Press; 1987.
[28] Munk P. Introduction to macromolecular science. New York: Wiley; 1989.